

March 3, 2018

## 1 Introduction

In order to conserve angular momentum, the probability that a nucleus relaxing toward the ground state will emit a photon in a given direction is dependent on the angle between the direction of emission and the spin axis of the nucleus [1]. When studying a free nucleus, the nuclear spin axis is free to rotate in space and thus  $\gamma$  emissions are isotropic. If relaxation proceeds through successive  $\gamma$  emissions however, the two emissions will be angularly correlated if there isn't enough time for the projection of the nuclear spin to be perturbed and rotated by extra-nuclear fields in between the two emissions. The aim of this paper is to verify the angular correlation expected from the  $\gamma$ - $\gamma$  cascade of decaying  $^{60}_{27}\text{Co}$ . To do so, a FAST-SLOW coincidence circuit was initially set up and the  $\gamma$  spectrum of a  $^{60}_{27}\text{Co}$  sample was measured. The number of angularly correlated photons for different angles were then measured.

## 2 Theory

A more detailed treatment of the theory of the angular correlation of nuclear radiation is provided in chapter XIX of [1]. Figure 1 shows the decay scheme of the sample used. The  $^{60}_{27}\text{Co}$  with half-life of  $\approx 5.3$  years decays via  $\beta^-$ -radiation into  $^{60}_{28}\text{Ni}$  with highest probability to the  $4^+$  angular momentum state. The Ni then relaxes to the ground state with the largest branching ratio being the  $4^+ \rightarrow 2^+ \rightarrow 0^+$  decay, producing two  $\gamma$  photons with respective energies of 1.17 and 1.33 MeV. The lifetime of the intermediate  $2^+$  Ni state is on the order of 1 ps which is too short to be perturbed by extra-nuclear fields and thus allowing for the angular correlation treatment. Decaying to the ground state follows via emitting one or more  $\gamma$  photons. The relaxing process with the largest branching ratio is the  $4^+ \rightarrow 2^+ \rightarrow 0^+$  decay, produces two  $\gamma$  photons. The corresponding lifetimes are short enough for the emissions to be considered coincidental (from the detecting electronics point of view), and for the assumption that extra-nuclear forces do not cause perturbation in the correlation between the photons. As the direction of the emission of the first photon is encoded with information on the projection of the spin axis of the nucleus due to angular momentum conservation, the probability of the direction of emission of the

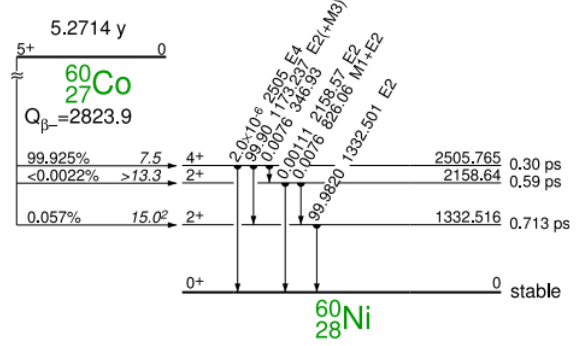


Figure 1:  $^{60}_{27}\text{Co}$  decay scheme [3]

second photon depends on the direction of the first emission. Thus, there is an angular correlation between the directions of the two  $\gamma$  emissions, given by the following directional correlation function for the  $\gamma$ - $\gamma$  cascade herein considered:

$$W(\theta) = 1 + A_{22}P_2(\cos \theta) + A_{44}P_4(\cos \theta),$$

where  $P_2$  and  $P_4$  are Legendre Polynomials,  $A_2 = 0.1020$ , and  $A_4 = 0.0091$  [1].

## 3 Experimental setup

The design of the apparatus is shown in Figure 2. The

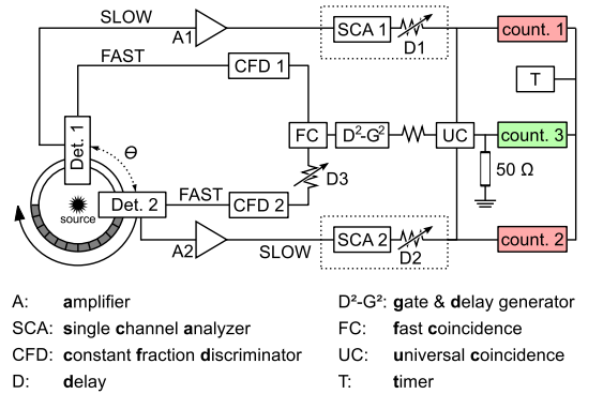


Figure 2: Experimental setup [2]

slow circuits count the number of photons incident to

the respective detectors which have energies within energy range set by the respective single channel analyzers. The slow circuit is used to only count the number of  $\gamma$  photons from the relevant  $\gamma$ - $\gamma$  cascade that are incident to the detectors within a time range set by the timer. The fast coincidence circuit counts the number of pairs of photons which arrive at the two detectors within a time window set by the fast coincidences unit. This circuit is used to distinguish and count pairs of photons which come from single  $\gamma$ - $\gamma$  cascade events as opposed to pairs of photons from two different cascade events. Though some random coincidences are still inevitably measured due to the large number of  $\gamma$ - $\gamma$  cascade events occurring at a given time in the sample, these random coincidences are eventually accounted for, as will be discussed in Section **WHERE?!?!?!?!?!.** The number of coincident photons from the fast and slow circuits are then matched by the universal coincidence unit to count the number of pairs of photons with the right energies and within the right time frame to be labelled as coming from single  $\gamma$ - $\gamma$  cascade events.

### 3.1 Detector

The detectors consist of a crystal scintillator and a photomultiplier as show in Figure 3. The scintillator absorbs the  $\gamma$ -ray and re-emits visible light in form of scintillation, which induces electron emission in the photomultiplier via the photoelectric effect. The high voltage provided between the (photo-)cathode and the anode accelerate the electron, which induces an avalanche of electrons by colliding with each of the dynodes. The signal produced by the PMT has a measurable height which is proportional to the energy of the incident photon. This signal is then input to the constant fraction discriminator in the fast circuit to measure the arrival time of the incident photon. As this procedure distorts the signal shape, which is required for the measurement of the energy of the incident photon, the output pulse cannot be used to measure the energy. Instead, an undistorted signal from an earlier phase of the amplification process is used as the input for the single channel analyzer in the slow circuit. It should be noted that Compton scattering also occurs in the scintillator which distorts the measured energy spectrum by producing a range of photons which are lower in energy than the incident photons. That said, peaks in the spectrum corresponding to the energy of the incident photons should still be easily observable above this Compton noise.

### 3.2 Constant Fraction Discriminator

The constant fraction discriminators modify the signals as seen in Figure 4: an attenuated inverted copy of the input is added to the delayed input signal. The resulting shape crosses the 0 V line ("zero crossing point"). This point serves as a time stamp for the signal which

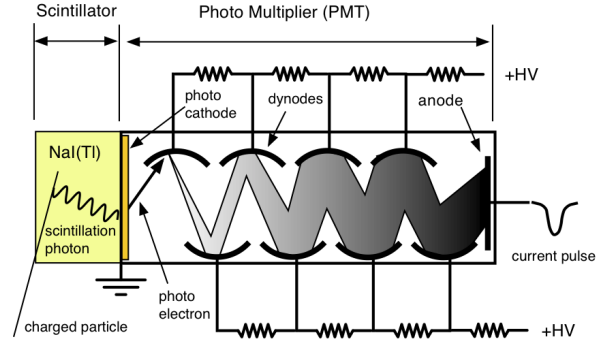


Figure 3: Scintillation detector with photomultiplier [4]

does not depend on the amplitude of the signal. The dis-

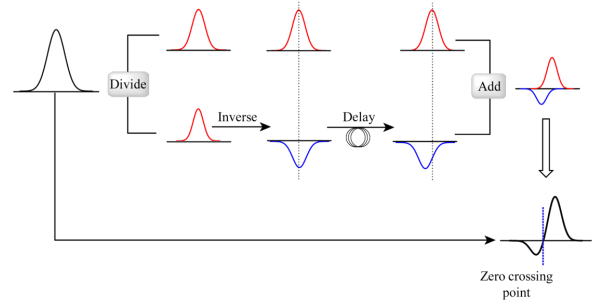


Figure 4: Scintillation detector with photomultiplier [5]

criminator has two outputs: the "fast" output which is a negative digital pulse and the "slow" output which is a positive one. The latter is used by the fast coincidence unit **FC**.

### 3.3 Single Channel Analyzers

The weak detector signal coming from the earlier dynode is fed through the amplifiers **A1** and **A2** first. The analyzers **SCA1** and **SCA2** determine whether the amplitudes of the signals, which are proportional to the energy of the  $\gamma$  photons, fall into an interval set by the **SCAs** with adjustable upper and lower limits.

### 3.4 Universal coincidences

The output signals from the **SCAs** and the **FC** are sent to the universal coincidence unit **UC** to count the total number of coincident photons. The signals from the **SCAs** are first sent through delays to make sure the signals incident to the **UC** correspond to photons hitting both detectors at the same time. The output from the **FC** is fed to a gate & delay generator **D<sup>2</sup>-G<sup>2</sup>** which delays the fast signal to ensure that the fast coincidences are correctly assigned to the right photons measured in the slow circuit when fed into the **UC**. Thus, the **UC**

counts the total number of photons which had the right energy and arrived within a short enough time frame expected from the  $\gamma$ - $\gamma$  cascade events.

## 4 Procedure

### 4.1 Amplifiers, constant-fraction discriminators

First the amplifiers  $A_1$ ,  $A_2$  were adjusted. We changed the gain using an oscilloscope such that the peaks corresponding to different detected photon energy levels don't hit the 9 V output ceiling of the amplifiers. The result of the adjustment is shown on Figure 7. Next we set the threshold of constant-fraction discriminators above the noise level by using the output of the CFD as the trigger for the amplifier signal of the same detector, increasing the threshold until the bright line at 0 V showing no photon detection (e.g. noise) disappeared.

### 4.2 Fast coincidence circuit, prompt curve

We connected the CFDs' positive outputs to the fast coincidence unit **FC**, one of them through a delay unit **D3**. Keeping the resolution time of **FC** at 15 ns, we used one of the counter units and changing the delay of **D3** to measure the coincidental detections as the function of the delay. We measured for  $(10.0 \pm 0.1)$  s for each delay value.

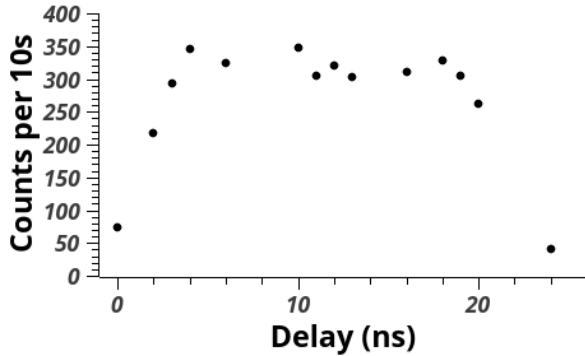


Figure 5: The measured prompt curve.

### 4.3 Angular correlation

After looking at the detector spectra, we chose the windows 520–720 (detector 1) and 540–740 (detector 2).

We measured the accidental coincidences overnight.

We used linear interpolation to get values for  $Q_2$  and  $Q_4$ . We chose the arithmetic mean of the two decay energies taken from [3], namely

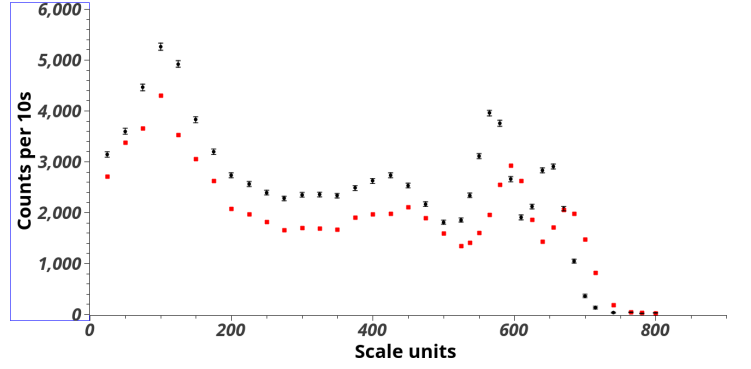


Figure 6: Measured detector spectra.

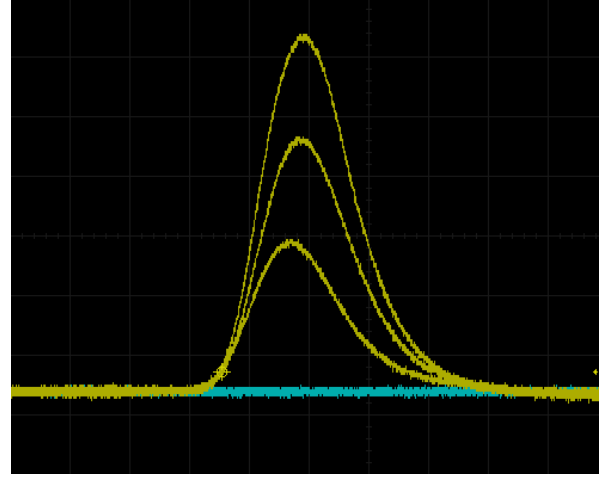


Figure 7: Well-adjusted signal of the amplifiers on channel 1 (yellow). A too high gain would cause the highest peaks to flatten as saturation happens before reaching the maximum.

$$E_{\text{avg}} = \frac{2505.765}{2} \text{ MeV} = 1252.8825 \text{ MeV}$$

With this,

$$Q_2(E_{\text{avg}}) \equiv Q_2^* = 0.962297$$

$$Q_4(E_{\text{avg}}) \equiv Q_4^* = 0.878188$$

We tried fitting a function of the form

$$W(\theta) = A(1 + B(Q_2^*)^2 \cos^2 \theta + C(Q_4^*)^2 \cos^4 \theta)$$

using the least-squares-fit method, which resulted in

$$A = 3604.19 \pm 30.69$$

$$B = 0.1157 \pm 0.0507$$

$$C = 0.04381 \pm 0.05732$$

The theoretical values of  $B$  and  $C$  ( $A$  is a scaling factor depending on the measurement time):

$$B_{\text{th}} = \frac{1}{8} = 0.125$$

$$C_{\text{th}} = \frac{1}{24} = 0.041\bar{6}$$

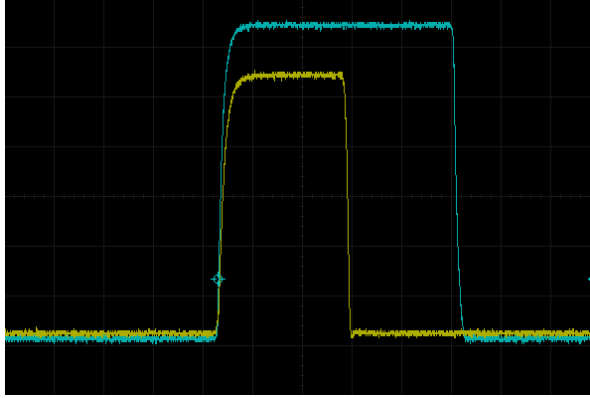


Figure 8: Adjusting the delay of the SCAs such that the leading edges of the signals from one SCA (yellow) and the gate and delay generator coincide.

## References

- [1] K. Siegbahn, ALPHA-, BETA-, AND GAMMA-RAY SPECTROSCOPY, Vol. 2, North Holland Publishing Company, Amsterdam (1965).
- [2] Booklet.
- [3] R. B. Firestone, Table of Isotopes 8<sup>th</sup> edition (Wiley, New York, 1996)
- [4] [http://wanda.fiu.edu/teaching/courses/Modern\\_lab\\_manual/scintillator.html](http://wanda.fiu.edu/teaching/courses/Modern_lab_manual/scintillator.html)
- [5] [https://en.wikipedia.org/wiki/Constant\\_fraction\\_discriminator#/media/File:Operation\\_of\\_a\\_CFD.png](https://en.wikipedia.org/wiki/Constant_fraction_discriminator#/media/File:Operation_of_a_CFD.png)

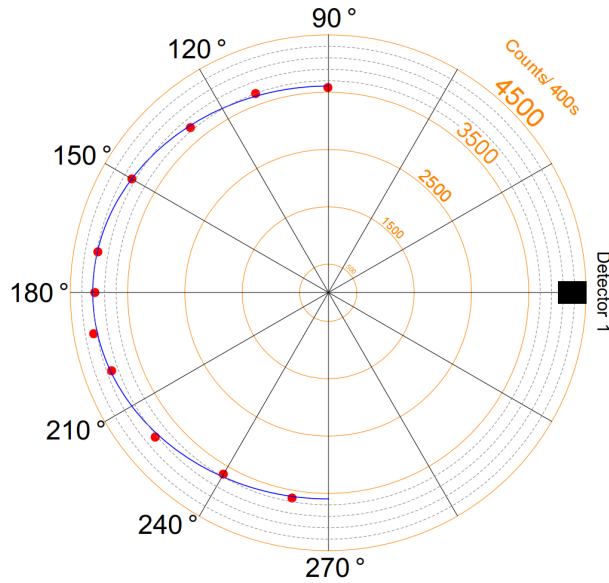


Figure 9: Polar plot of angular correlation. Red: the measured values (uncertainties not shown). Blue: the acquired fitting.